

# The Chromospheric Solar Millimeter-wave Cavity, as a Result of the Temperature Minimum Region

Victor De la Luz<sup>1,2</sup>, Jean-Pierre Raulin<sup>3</sup>, Alejandro Lara<sup>2</sup>

Received \_\_\_\_\_; accepted \_\_\_\_\_

Not to appear in Nonlearned J., 45.

---

<sup>1</sup>Instituto Nacional de Astrofísica, Óptica y Electrónica, Tonantzintla, Puebla, Mexico, Apdo. Postal 51 y 216, 72000.

<sup>2</sup>Instituto de Geofísica, Universidad Nacional Autónoma de México, México, 04510.

<sup>3</sup>CRAAM, Universidade Presbiteriana Mackenzie, São Paulo, SP, Brasil, 01302-907.

## ABSTRACT

We present a detailed theoretical analysis of the local radio emission at the lower part of the solar atmosphere. To accomplish this, we have used a numerical code to simulate the emission and transport of high frequency electromagnetic waves from 2 GHz up to 10 THz. As initial conditions we used VALC, SEL05 and C7 solar chromospheric models. In this way, the generated synthetic spectra allows us to study the local emission and absorption processes with high resolution in both altitude and frequency.

Associated with the temperature minimum predicted by these models we found that the local optical depth at millimeter wavelengths remains constant, producing an optically thin layer which is surrounded by two layers of high local emission. We call this structure the Chromospheric Solar Millimeter-wave Cavity (CSMC). The temperature profile which features the Temperature Minimum layers and the following Temperature rise produces the CSMC phenomenon.

The CSMC show the complexity of the relation between the theoretical temperature profile and the observed brightness temperature and may help to understand the dispersion of the observed brightness temperature in the millimeter wavelength range.

*Subject headings:* radiative transfer equation, solar radio emission, numerical model

## 1. Introduction

The necessity of a two component (hot and cold) model to explain the chromospheric solar observations was established by Giovanelli (1949). A low temperature zone in the chromosphere was inferred by observations in different regions of the solar spectrum in both, line-emission (e. g.: H and K of *CaII* in the Visible; *Mg h* and *k* resonance lines in the UV) and continuum (e.g.; the 135-168 nm in UV and the 33-500  $\mu\text{m}$  in microwave ranges). Moreover, by observing emission lines (*Fe*, *Si*, *K1* of *CaII*, and *k1* of *Mg*) at the disk center, the height of the low temperature region was set at the lower part of the chromosphere, very close to the photosphere (Athay 1970).

A considerable advance in the understanding of the chromosphere was obtained by the so called VAL models. Using these models and based on adequate spatial resolution observations, Vernazza et al. (1973, 1976, 1981) found that a minimum of temperature can be modeled by assuming a plane-parallel atmosphere in hydrostatic equilibrium and considering Non-Local Thermodynamic Equilibrium (NLTE). After that, Fontenla et al. (1990) improved the VAL models by including several updates (both observationally and theoretically); the most important being the ambipolar diffusion which removed the “plateau” of temperature in the high chromosphere.

The most recent and advanced model is the so called “C7 model” (Avrett & Loeser 2008) which also follows the common assumptions of Vernazza et al. (1973). In particular, this model predicts that the continuum emission at 500  $\mu\text{m}$  comes from the region where the temperature reaches its minimum value. The temperature minimum region has been set by the mentioned semi-empirical models at heights ranging between 400 and 600 km above the photosphere (Kuznetsova 1978; Ahmad & Kundu 1981; Vernazza et al. 1981; Fontenla et al. 1990; Avrett & Loeser 2008). In the literature we also found purely empirical models, for example the SEL05 model (Selhorst et al. 2005) that closely matches the observations made

by Ewell et al. (1993); Kuseski & Swanson (1976); Beckman et al. (1973); Linsky (1973).

Despite the fact that the chromosphere (where reaches the temperature minimum) plays a fundamental role in the dynamics and heating of the upper atmosphere (acting as the interface between the lower photospheric layers where  $\beta$ , the ratio between the dynamic and magnetic pressures is much higher than one and the higher dynamic atmosphere where  $\beta \ll 1$ ), this layer is not well understood. Recently a renewed interest on this fundamental layer has grown due to the advent of better observational and reconstruction technics applied to ground based as well as space borne telescopes giving access to high space and time resolution observations of the solar chromosphere.

In this context, the analysis of the aforementioned models predicts that the millimeter and sub-millimeter (7.5 to 0.75 mm) quiescent solar emission comes from a layer in the lower chromosphere related to the temperature minimum (Vernazza et al. 1981).

It is well established that the height and width of a radio emitting layer can be characterized using radiative transport models (Avrett & Loeser 2008). However, in general these analysis consider only the upper layer (or final boundary) of the emission region, i.e. the layer where the atmosphere becomes optically thick. Therefore, the knowledge and understanding of the local emission produced at lower layers remains neglected. Note that the fact that these regions are not easily accessible to radio telescopes, does not prevent us to study the possible physical processes occurring inside them. To overcome these limitations, in a previous analysis of the quiet chromosphere, we have explored the local emission at 17, 212, and 405 GHz frequencies and found that there are two main regions of emission, the first one is close to the photosphere and the second is located at  $\sim 1000$  km over the photosphere (De la Luz et al. 2011).

In the present work we continue to study the local radiative transfer processes in different layers of the atmosphere (we present a brief description of the model in Section 2,

for details see De la Luz et al. 2011), for the empirical model SEL05 and two semi-empirical models: C7 and VALC (Section 3), but extend it to a larger range of frequencies, from 2 GHz to 10 THz (Section 4). In particular, we study the radio emission associated with the minimum of temperature and the lower chromosphere (Section 5).

It worth to mention that the study of the solar spectrum morphology, specially at sub-millimeter and infrared wavelengths, is also important for studies of dusty circumstellar disks (Zuckerman 2001) because the emission from the chromosphere of main-sequence solar-like stars at these wavelengths could be comparable with that emerging from circumstellar material.

## 2. Radio Emission Model

In order to compute the radio emission, we solve locally the radiative transfer equation. The amount of energy  $dI_\nu$  passing through volume element characterized by the length  $ds$  is equal to the absorption  $I_\nu\kappa_\nu$  plus the emission  $\epsilon_\nu$  inside the element, this is:

$$\frac{dI_\nu}{ds} = -I_\nu\kappa_\nu + \epsilon_\nu \quad (1)$$

where  $\kappa_\nu$  is the opacity function and  $\epsilon_\nu$  is the emission function. The solution of the radiative transfer equation can be represented in a local cell as follows:

$$I_{lcl} = \epsilon_{abs} + \epsilon_{emi}, \quad (2)$$

where  $I_{lcl}$  is also know as the contribution function (Gray 1976), and

$$\epsilon_{abs} = I_0 \exp(-\tau_{lcl}) \quad (3)$$

is the local absorption and

$$\epsilon_{emi} = S_{lcl}(1 - \exp(-\tau_{lcl})) \quad (4)$$

is the local emissivity. In this case,  $I_0$  is the incoming radiation,  $\tau_{lcl}$  is the local optical depth and  $S_{lcl}$  is the local source function. We remind the reader that the specific intensity,  $I_\nu$ , can be converted to brightness temperature,  $T_b$ , using the Rayleigh-Jeans approximation:

$$I_\nu = \frac{2k\nu^2 T_b}{c^2}, \quad (5)$$

where  $c$  is the speed of light and  $k$  is the Boltzmann constant. Then we can re-write equation (2) using

$$T_{bcl} = \frac{I_{lcl} c^2}{2k\nu^2}, \quad (6)$$

where  $T_{bcl}$  is the local brightness temperature.

In order to characterize the local efficiency emission and absorption of the atmosphere, we define:

$$E_l = 1 - \exp(-\tau_{lcl}) \quad (7)$$

as the local efficiency of emissivity and

$$A_l = \exp(-\tau_{lcl}) \quad (8)$$

as the local efficiency of absorbance. The values for  $E_l$  and  $A_l$  can vary between 0 and 1, where 0 means optically thin and 1 optically thick.

Using the local emissivity and absorbance, we compute iteratively the emission over a ray path by solving the radiative transfer equation (De la Luz et al. 2010). Finally, the total emission efficiency, in the altitude range ( $\xi$ ) from  $h_1$  up to  $h_2$ , is:

$$\epsilon_T(h_1, h_2) = 1 - \exp\left(-\sum_{\xi=h_1}^{h_2} \tau_{lcl}(\xi)\right) = 1 - \exp(-\tau(h_1, h_2)) \quad (9)$$

where  $\tau(h_1, h_2)$  is the optical depth between  $h_1$  and  $h_2$ .

### 3. The Solar Chromospheric Temperature Profiles

The temperature structure in the Sun, and in general, in stars, decreases monotonically with stellar (solar) radius. In the case of the Sun, more elaborated models that include chromospheric heating (Vernazza et al. 1981; Selhorst et al. 2005; Avrett & Loeser 2008, VALC, SEL05, and C7 model respectively) indicate that the temperature reaches a minimum value at about 400 and 600 km above the solar photosphere (Figure 1). Above this point, the temperature gradually increase up to coronal temperatures ( $\approx 1$  MK).

A comparison among the three above mentioned models show only marginal differences in the temperature profile, but quite significant discrepancies at greater heights, including the value of the temperature minimum. For instance, the VALC model predicts that the temperature at the minimum ( $T_{min}$ ) is 4170 K, and is located at 515 km above the photosphere. Similarly the models C7 and SEL05 place the minima at 560 ( $T_{min} = 4400K$ ) and 500 km ( $T_{min} = 4407K$ ), respectively.

By inspection of Figure 1 one can see that the results from the three models intersect at about 900 km. Above this point, the models behave differently: The SEL05 profile increases linearly with height until 7700 K, while the VALC model increases from 5800 to 7200 K but not linearly, C7 grows from 5800 to 6650 K where remains almost constant for the next 800 km. Finally, the VALC model presents a plateau in temperature (around 24500 K) between 2115 km and 2267 km.

In the Figure 2 we plot the differences in the radial temperature profiles between the three models, taking as a reference the C7 model. We found three heights where the differences in temperature are higher than 6%: around 400 km (6% only the VALC model), 750 km (8.5%), and 1100 km (6%). In these cases the differences with the C7 model are significant but always less than 10%.

#### 4. Synthetic Spectrum

We use PakalMPI (De la Luz et al. 2011), an update version of the Pakal code (De la Luz et al. 2010) to compute a synthetic spectrum of the solar emission from millimeter to infrared wavelengths (from 2 GHz to 10 THz). PakalMPI solves the radiative transfer equation with NLTE conditions, in a three dimensional geometry using a multiprocessor environment. As model of emission, we use “Celestun” which includes three opacity functions in the continuum: Bremsstrahlung (Rybicki & Lightman 1986), Neutral Interaction (John 1988; Zheleznyakov 1996) and Inverse Bremsstrahlung (Golovinskii & Zon 1980). Celestun model, also includes ionization stages of twenty ion species considering  $H$ ,  $H^-$ , and  $n_e$  in NLTE (see De la Luz et al. 2011, for more details). The input parameters of PakalMPI are physical quantities as temperature, Hydrogen density and metalicity. These parameters are taken from an atmospheric model, in this case the VALC, SEL05, and C7 models mentioned in the previous section.

In the Figure 3 we shows the differences between the final brightness temperature (synthetic spectrum) for the three models taking as reference the C7 model. We show that below 90 GHz the differences between C7 and the VALC models exceed 20%. The comparison between C7 and SEL05 show differences of 30% or less in all the frequency range under study, being around 8, 200 and 1200 GHz the points in frequency that presents very similar brightness temperatures.

Figure 4 show the computed optical depth ( $\tau$  in equation 9) for each model at 10, 40, 200, and 800 GHz. For the C7 and the VALC models, between 480 and 1000 km over the photosphere (marked with vertical lines), the optical depth remains roughly constant. In other words,  $\tau_{lcl}$  is very small and the local emissivity is negligible (equation 4).

Using the SEL05 model, the local optical depth presents two steps in the same region. This is due to the fact that this model has an artificial peak enhancement of the Hydrogen



density which causes an increment of the opacity at  $\sim 600$  km over the photosphere (Figure 5). This artificial peak also modifies the total and local efficiency. This region with Hydrogen over-density is a consequence of the fully ionized gas approximation used in the SEL05 model, which is not applicable at the low chromosphere (De la Luz et al. 2011).

The Figure 6 show the contour plot of the total emission efficiency (equation 9) as a function of frequency and height for the C7 model. In particular we are interested in the Interface between Optically Thick and Thin region (*IOTT*). The interface can be defined as the region in height where the emission efficiency is  $0.9 > \epsilon_T > 0.1$ .

This region is presented in the plot as the gradient ribbon between red (optically thick) and blue (optically thin) colors. We want to remark that the final brightness temperature comes from the total optical depth and is related with the total emission efficiency. The analysis of the local emission and absorption process help us to understand the local emission and absorption process although remains hidden in the observations.

In the case of the C7 model one can see that the 10 GHz emission comes from a layer situated at about 2100 km above the photosphere. Whereas the 100 GHz source is located at 1500 km above the photosphere. The *IOTT* in the 2 - 500 GHz frequency range is located in a large range of heights, between 1000 and 2100 km above the photosphere. On the other hand, inside the 500 - 2000 GHz frequency range, the *IOTT* remains roughly constant with altitude, from 500 to 1000 km. This is a direct consequence of the optical depth “Plateau” showed in Figure 4.

The results for the VALC model are very similar to these obtained using the C7 model. We can see a slowly decreasing of the *IOTT* between 10 and 300 GHz, then an abrupt change around 400 GHz is observed.

At low frequencies, both C7 and VALC models predict a very low, and therefore

unrealistic, altitude of the emitting sources. This is due to the fact that these models do not take into account the Corona and the Transition Region.

For the SEL05 model, the effect of the Hydrogen over-density in the emission efficiency is seen as a rapid shift of the *IOTT* towards higher frequencies at  $\sim 600$  km of height over the photosphere, where the peak of Hydrogen is located (Figure 5). In this case, the inclusion of ad-hoc Coronal physical conditions produces an increment in the altitudes of the low frequency sources ( $< 30$  GHz), giving more realistic results for this range of frequencies than the models without Corona (C7 and VALC models).

In the Figure 5 from De la Luz et al. (2011), we can observe the brightness temperatures computed with these models and their comparison with the observations (collected by Loukitcheva et al. 2004). This figure show that SEL05 provides the best match (although their approximation in the low chromosphere disagree with the semi-empirical models predictions). The results of C7 and VALC models presents opposite behaviors. At lower frequencies the predicted brightness temperature differs of the observations, C7 show lower and VALC higher brightness temperatures in the same range of frequencies. This situation is partially inverted around 400 GHz where both models shows brightness temperature above the observed but C7 predicts higher brightness temperatures than VALC. If we observe the Figure 2, a direct relation between the differences in the radial temperature models and the final brightness temperatures can not be easy established.

## 5. The Chromospheric Millimeter-wave Cavity

De la Luz et al. (2010, 2011) reported that the emission profiles, in the 40 to 400 GHz range, have two regions of enhanced local emissivity. Remarkably, no attention has been paid early to this interesting behavior. For instance, in figure 2 from Avrett & Loeser

(2008), we note that at 0.5 mm there are also two regions of emission, unfortunately the authors did not elaborate much on this result. In this work we present a detailed study of this region.

We show in Figure 7 the contour plot of the local emission efficiency (equation 7) as a function of frequency and height for the C7 model, where  $E_l$  varies from optically thin (blue) to optically thick (red) medium. There is a peculiar zone of low emissivity centered at about  $\sim 750$  km above the photosphere. This atmospheric zone forms a cavity starting at  $\sim 40$  GHz; its width grows with frequency; and ending at  $\sim 400$  GHz.

Between 40 and 400 GHz the cavity, surrounded by two zones of enhanced local emission is clearly seen. At a given frequency within this range (for instance 100 GHz), and moving outward from the photosphere, we first find a region where the atmosphere emits efficiently (in red color between 0 and 600 km), then there is a region where the atmosphere becomes thinner (in blue color between 600 and 900 km) and finally, a second region of emission appears (red color between 900 and 1300 km), i. e. we have crossed three times the Local Interface between Optically Thick and Thin region ( $IOTT_l$ ), in this case defined as the region in height where the local efficiency of emissivity is  $0.9 > E_l > 0.1$ . The  $IOTT_l$  divided the synthetic spectrum in three regions: between 2 and 40 GHz (where cross one time through the  $IOTT_l$ ), the second region between 40 and 400 GHz (cross three times) and between 400 and 10000 GHz (cross one time).

The VALC and SEL05 models shows the same characteristic. The SEL05 model show a more complex structure, in particular it has a characteristic peak around 600 km over the photosphere, which has been discussed previously.

We call this region the Chromospheric Solar Millimeter-wave Cavity (CSMC). This is a region of the solar atmosphere where the opacity at millimeter and sub-millimeter wavelengths is reduced, surrounded by two zones of enhanced opacity. As far as we know,

the presence of the CSMC have never been studied or previously mentioned in the literature.

## Discussion and Conclusions

The optical thickness of the solar atmosphere depends of the opacity functions involved in the emission/absorption processes. At millimeter wavelengths the important processes are the neutral interaction and the classical Bremsstrahlung (De la Luz et al. 2011). These mechanisms depends of the temperature and the electronic and ion density.

In the chromospheric layers, close to the temperature minimum, the rate of ionization is low and therefore, the number of interactions between electron and ion decreases, resulting in locally thin atmospheric layers (at millimeter wavelengths). Around this region, the temperature raises producing free electrons and ions and therefore, these atmospheric layers become optically thick. The interplay between the optically thick and thin layers produces the Chromospheric Solar Millimeter-wave Cavity.

We knows (De la Luz et al. 2011) that the first 500 km over the photosphere the Neutral Interaction is the most important mechanism in the emission and absorption process then, the Bremsstrahlung comes the major contributor in the optical depth. The second region of emission in the CSMC begin around 700 km over the photosphere, we can concludes that the neutral interactions do not influence the resulting CSMC.

The morphology of the CSMC is a model-based phenomenon. In this work, we have used two well known semi-empirical models (VALC and C7) and one ad-hoc model (SEL05) and all of them showed the CSMC structure but with small changes in its morphology. We think that in average the used models reproduce well the physical conditions in the low chromosphere due that the computations in another regions of the spectrum show consistence (Vernazza et al. 1981; Avrett & Loeser 2008). However, the differences in the

computed synthetic spectra at millimeter, sub-millimeter and infrared regions should be taken into account not only to test the auto consistence of the models but as tool to improve the radial temperature profile.

The presence of the CSMC show that the relationship between the theoretical radial profile of temperature and the observed spectrum is complex, against the general idea of a simple linear relationship as suggested by Avrett & Loeser (2008). We think that the CSMC must be a intrinsic characteristic of the solar chromosphere and could help to understand better the brightness temperature spectrum from microwave to sub-mm range.

A comparison between the observations (collected by Loukitcheva et al. 2004) and the brightness temperature computed with C7 and VALC, predicts higher brightness temperatures (Figure 5 from De la Luz et al. 2011) in almost all the frequency range, except in the interval between 90 and 400 GHz. The SEL05 model fix better the same observations, but in this work, we shows that the SEL05 approximations causes inconsistencies in the Hydrogen density profile.

The  $IOTT$  and the  $IOTT_l$  define different frequency regions and heights of emission in the synthetic spectrum. The  $IOTT$  present three regions: 2 - 500 GHz, 500 - 2000 GHz, and 2000 - 10000 GHz while  $IOTT_l$  shows: 2 - 40 GHz, 40 - 400 GHz and 400 - 10000 GHz. Although the final brightness temperature is related directly with the  $IOTT$  the true responsible behind the shape spectrum is the  $IOTT_l$ , i.e. the CSMC.

We can concludes that to fix the high brightness temperature computed with C7 and VALC (after 400 GHz), we need decrease the local optical depth around the heights of the second peak of local emission of the CSMC. The opacity function at this altitudes mainly depends of the Bremsstrahlung process, i.e. lower temperatures than the published for C7 and VALC between 700 and 1500 km over the photosphere could decrease the local opacities values and then decrease the brightness temperature. In particular, we expect

that the sources of emission more sensitive to the CSMC are at frequencies between 400 and 600 GHz, where finish the second peak of emission of the CSMC. We expect that the height of the source of emission may vary between 500 and 1000 km over the photosphere, causing a large dispersion in the spectrum at this frequencies.

On the low part of the spectrum, the inclusion of Transition Region and Corona could fix the low brightness temperatures predicted by C7 at frequencies lowers than 40 GHz. The VALC plateau of temperature between 2115 and 2267 km over the photosphere is the responsible of the high brightness temperature computed with this model, in particular in the centimetric range. Sub-millimeter solar observations are needed in order to confirm the presence of the CSMC particularly between 400 and 600 GHz.

Finally, as the CSMC is a direct consequence of the minimum temperature layers (mostly of the gradual temperature rise in the low chromosphere), it could give new insights about the structure of the solar atmosphere, and also it can be extended to the case of solar-like stars.

Part of this work was supported by UNAM-PAPPIT IN117309-3 and CONACyT 24879 grants. Thanks to the National Center of Super-computing in Mexico for allow us to use there computer facilities, Dr. Emanuele Bertone and Dr. Miguel Chavez for useful comments. Thanks to Professor Pierre Kaufmann, director of CRAAM - Centro de Radioastronomia e Astrofisica Mackenzie, where part of this research was conducted. JPR thanks CNPq agency (Proc. 305655/2010-8).

## REFERENCES

- Ahmad, I. A., & Kundu, M. R. 1981, *Sol. Phys.*, 69, 273
- Athay, R. G. 1970, *ApJ*, 161, 713
- Avrett, E. H., & Loeser, R. 2008, *ApJS*, 175, 229
- Beckman, J. E., Clark, C. D., & Ross, J. 1973, *Sol. Phys.*, 31, 319
- De la Luz, V., Lara, A., Mendoza-Torres, J. E., & Selhorst, C. L. 2010, *ApJS*, 188, 437
- De la Luz, V., Lara, A., & Raulin, J.-P. 2011, *ApJ*, 737, 1
- Ewell, Jr., M. W., Zirin, H., Jensen, J. B., & Bastian, T. S. 1993, *ApJ*, 403, 426
- Fontenla, J. M., Avrett, E. H., & Loeser, R. 1990, *ApJ*, 355, 700
- Giovanelli, R. G. 1949, *MNRAS*, 109, 298
- Golovinskii, P. A., & Zon, B. A. 1980, *Zhurnal Tekhnicheskoi Fiziki*, 50, 1847
- Gray, D. F. 1976, *The observation and analysis of stellar photospheres*, ed. Gray, D. F.
- John, T. L. 1988, *A&A*, 193, 189
- Kuseski, R. A., & Swanson, P. N. 1976, *Sol. Phys.*, 48, 41
- Kuznetsova, N. A. 1978, *Soviet Astronomy*, 22, 345
- Linsky, J. L. 1973, *Sol. Phys.*, 28, 409
- Loukitcheva, M., Solanki, S. K., Carlsson, M., & Stein, R. F. 2004, *A&A*, 419, 747
- Rybicki, G. B., & Lightman, A. P. 1986, *Radiative Processes in Astrophysics* (*Radiative Processes in Astrophysics*, by George B. Rybicki, Alan P. Lightman, pp. 400. ISBN 0-471-82759-2. Wiley-VCH , June 1986.)

Selhorst, C. L., Silva, A. V. R., & Costa, J. E. R. 2005, *A&A*, 433, 365

Vernazza, J. E., Avrett, E. H., & Loeser, R. 1973, *ApJ*, 184, 605

—. 1976, *ApJS*, 30, 1

—. 1981, *ApJS*, 45, 635

Zheleznyakov, V. V., ed. 1996, *Astrophysics and Space Science Library*, Vol. 204, Radiation  
in Astrophysical Plasmas

Zuckerman, B. 2001, *ARA&A*, 39, 549



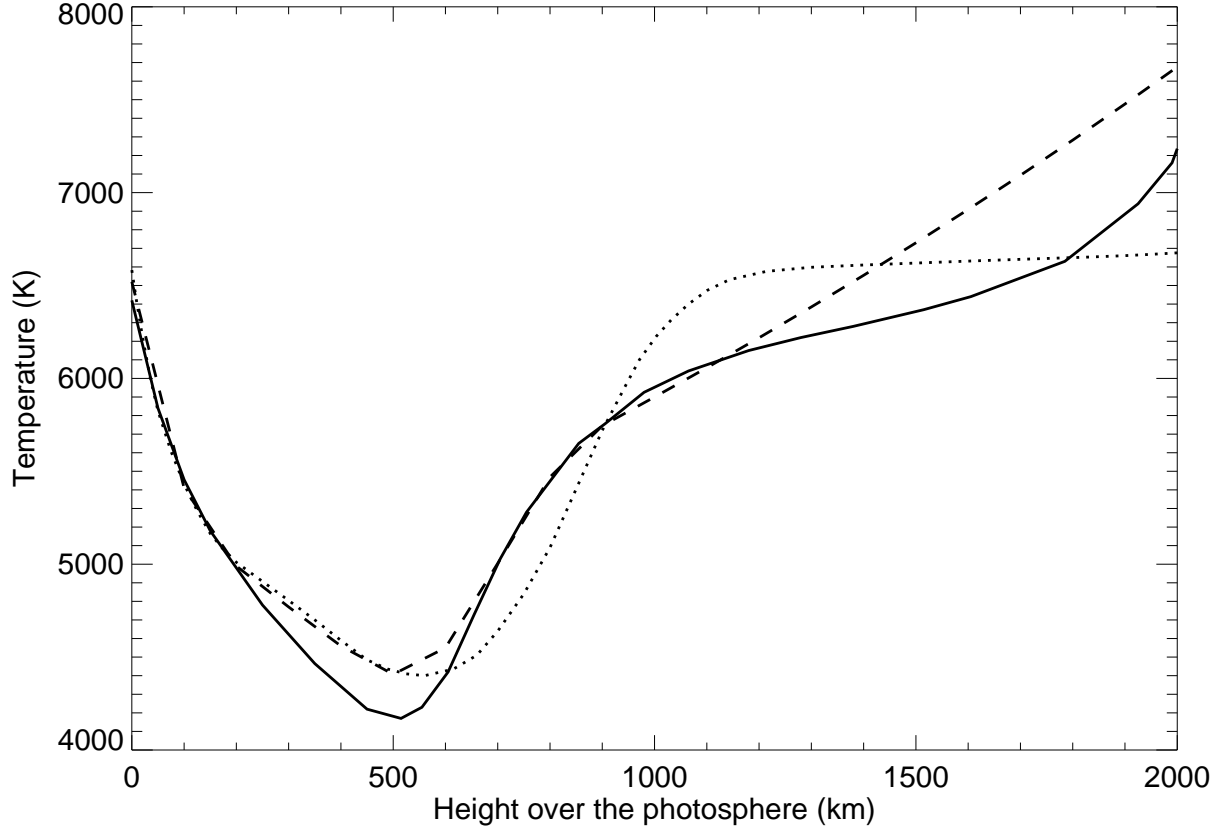


Fig. 1.— Radial temperature profiles of three Chromospheric models. The continuous line is the VALC model from Vernazza et al. (1981), the dashed line corresponds to the model of Selhorst et al. (2005) and the dotted line is the C7 model from Avrett & Loeser (2008).

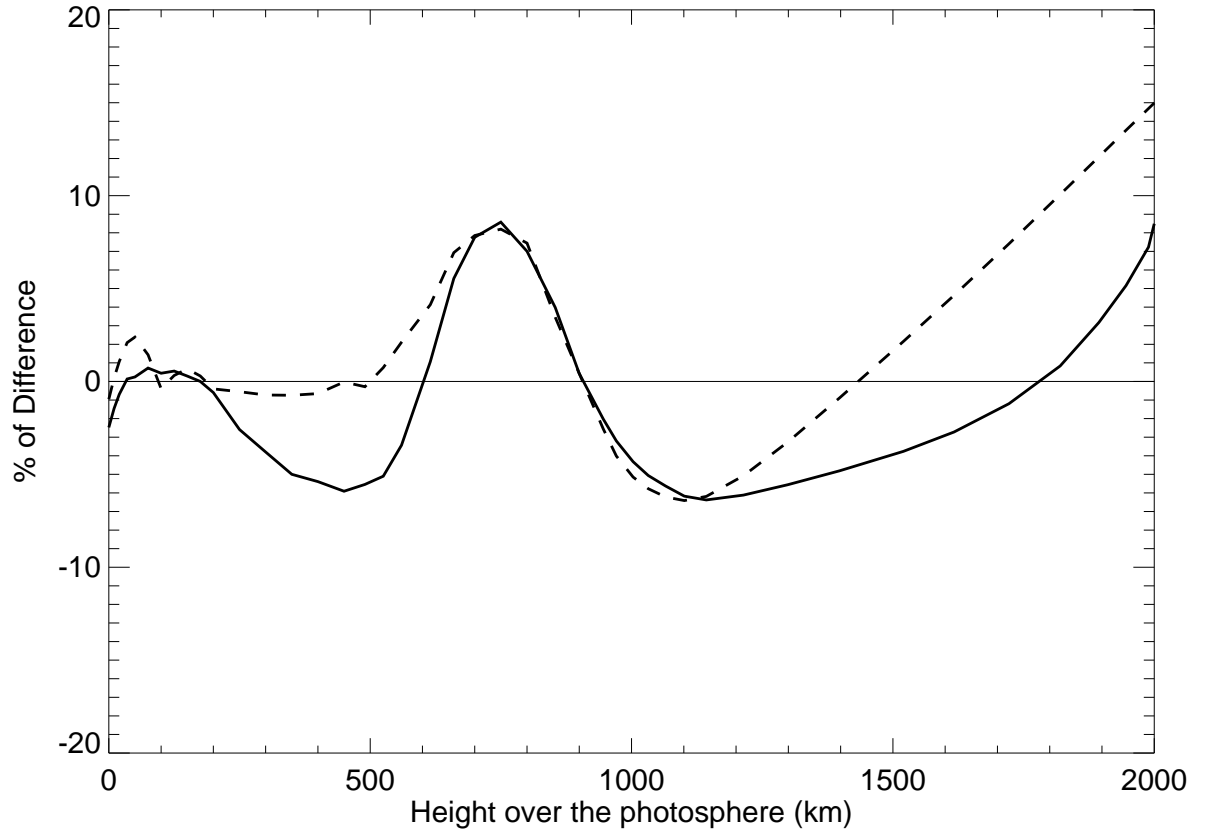


Fig. 2.— Difference in the temperature profile between the C7 model (taking as reference) and the VALC (continuous line) and SEL05 (dashed line) models.

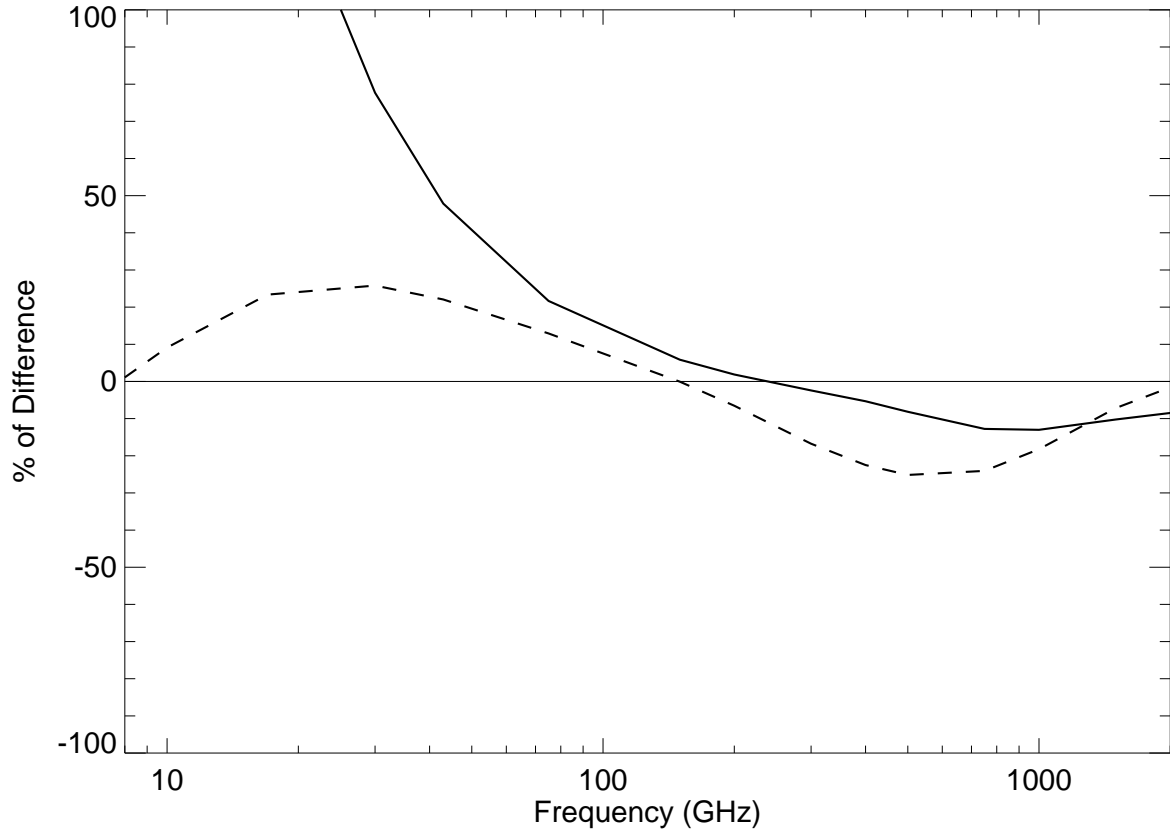


Fig. 3.— Difference in the brightness temperature between the C7 model (taking as reference) and the VALC (continuous line) and SEL05 (dashed line) models.

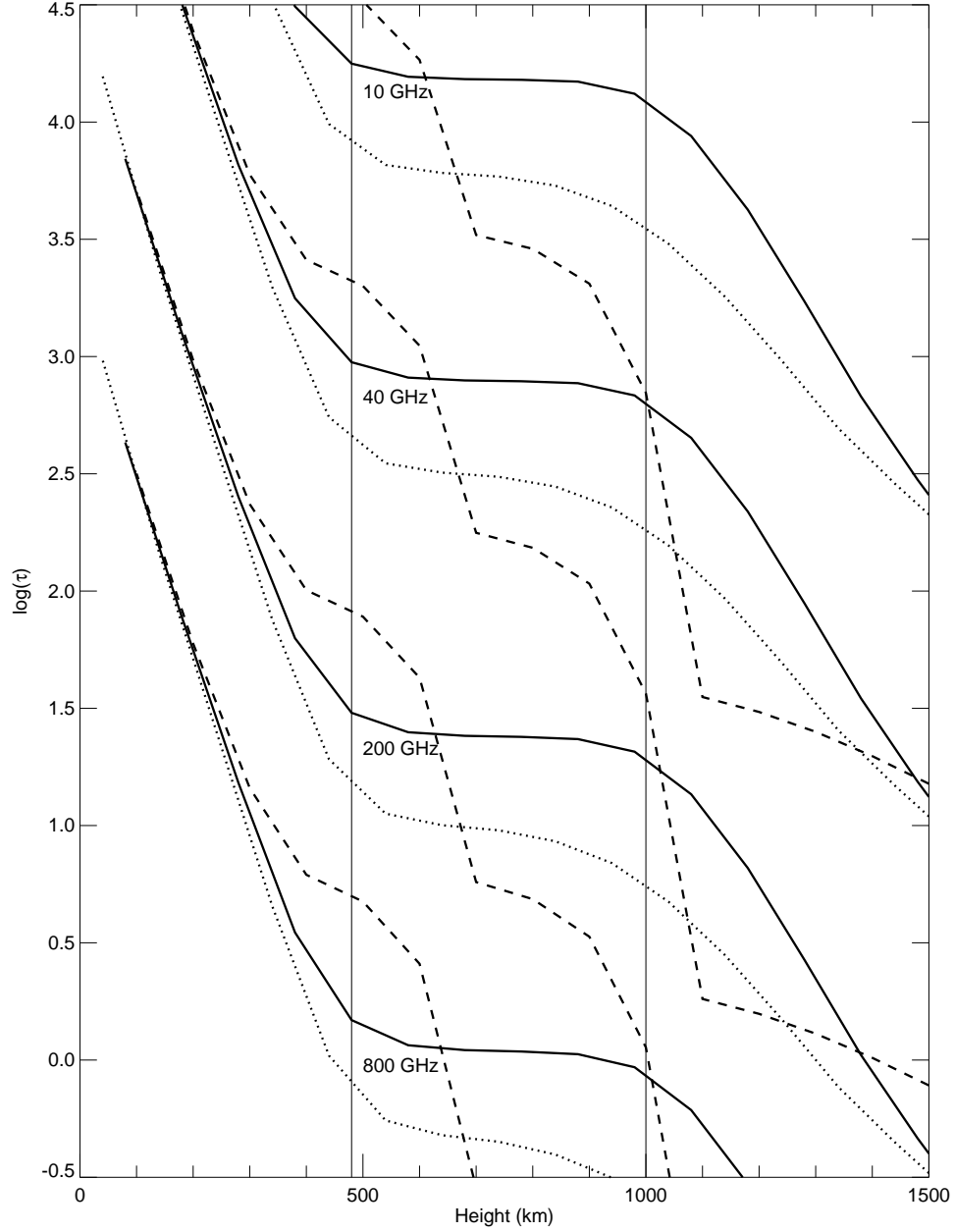


Fig. 4.— Optical depth computed for 10, 40, 200 and 800 GHz using the C7 (continuous line), VALC (dotted line), and SEL05 (dashed line) models. Note that the optical depth for the C7 and VALC models remains almost unalterable at heights between 480 and 1000 km over the photosphere, forming an optical depth Plateau.

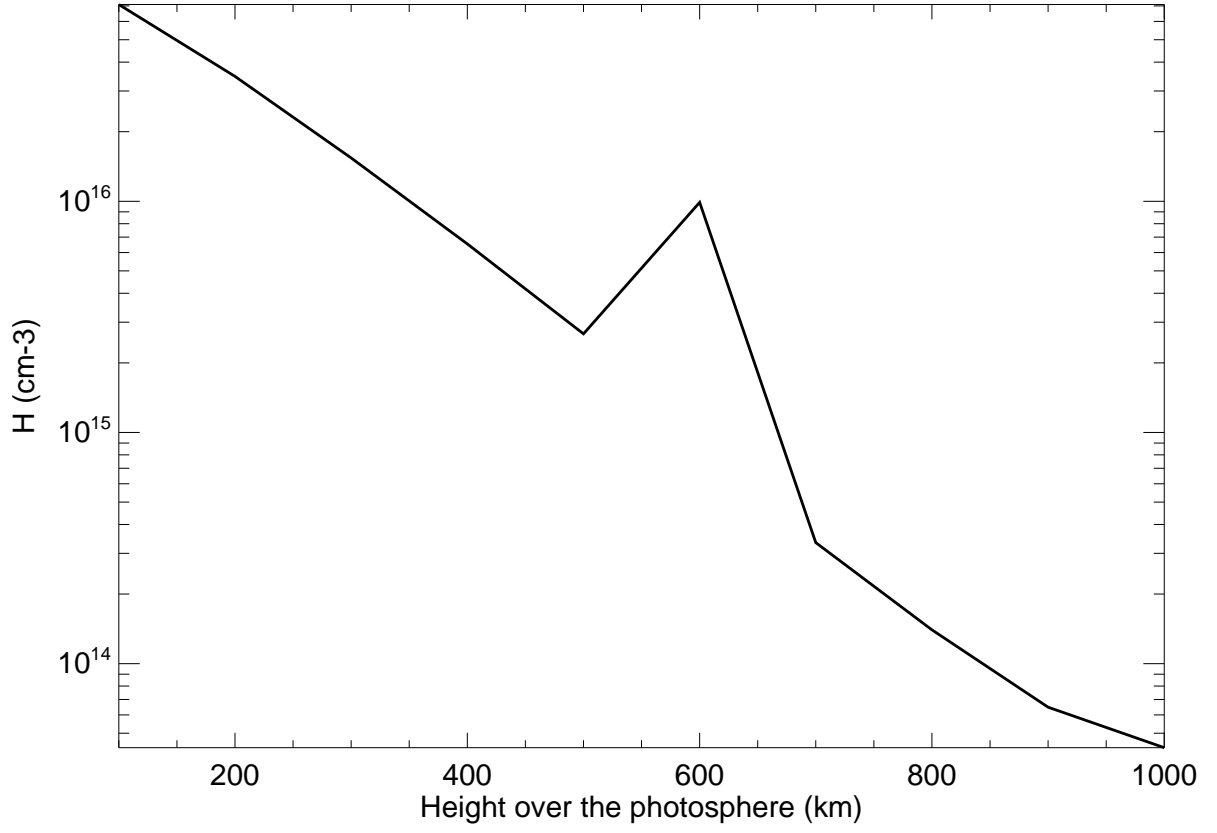


Fig. 5.— Hydrogen density profile from SEL05 model. The peak around 550 km is a consequence of the full ionized gas hypothesis.

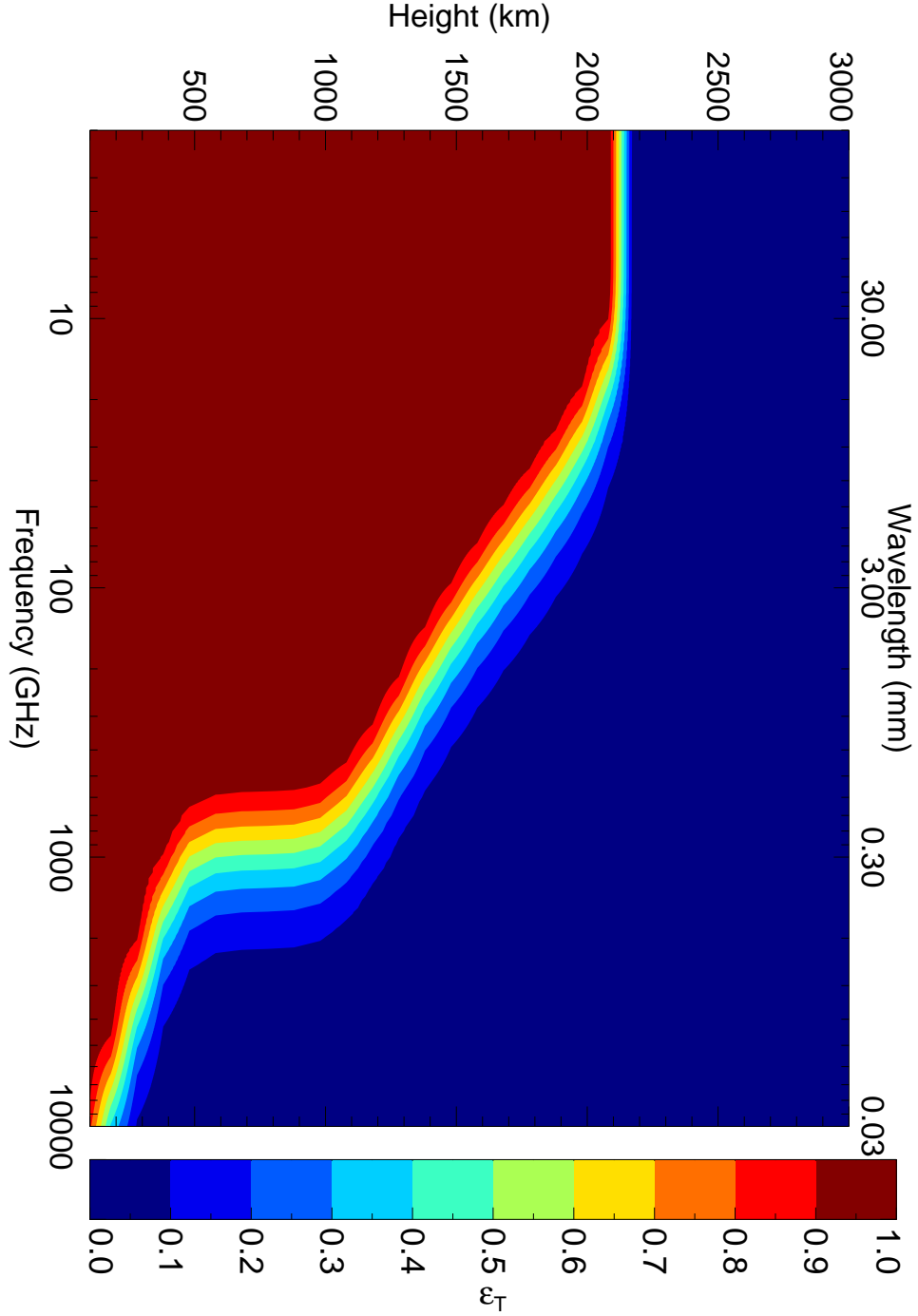


Fig. 6.— Synthetic solar spectrum from 2 GHz to 10 THz as a function of the atmospheric height over the photosphere. The contours correspond to the efficiency of the total emission ( $\epsilon_T$ ) computed using the C7 model (for this and the following figures blue means optically thin and red optically thick). The region between 500 and 200 GHz is an effect of the Optical Depth Plateau.

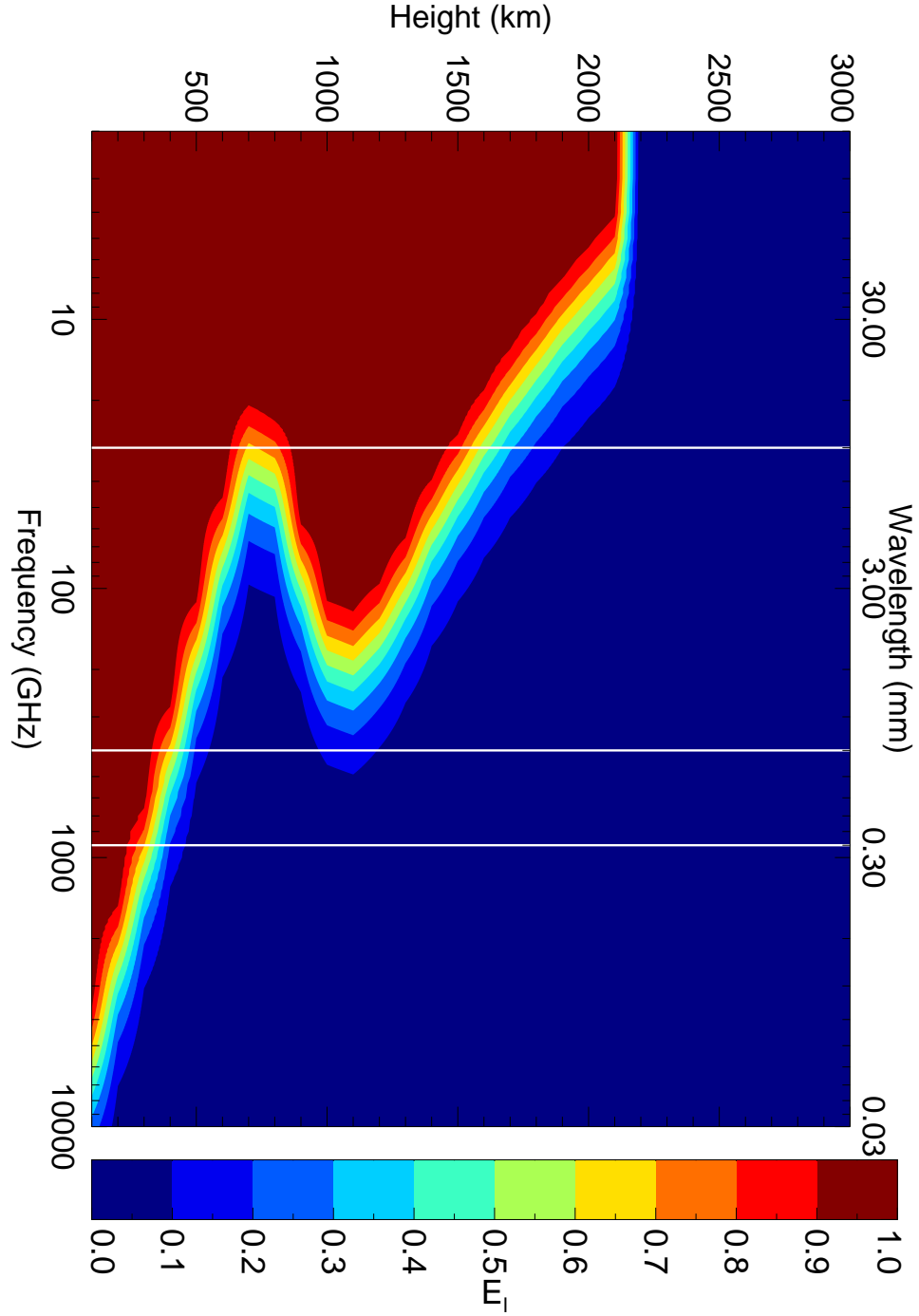


Fig. 7.— Contour plot of the local emissivity efficiency  $E_l$  computed using the C7 model. the white vertical lines mark the Chromospheric Solar Millimeter-wave Cavity (CSMC).